Thin-film transducers for the detection and imaging of Brillouin oscillations in transmission on cultured cells

2016 J. Phys.: Conf. Ser. 684 012003

(http://iopscience.iop.org/1742-6596/684/1/012003)

Journal of Physics: Conference Series **684** (2016) 012003 doi:10.1088/1742-6596/684/1/012003

Thin-film transducers for the detection and imaging of Brillouin oscillations in transmission on cultured cells

F Pérez-Cota[1], R J Smith[1], E Moradi[2], K Webb[2] and M Clark[1]

[1]Electrical Systems and Optics Research Division, University of Nottingham, University Park, Nottingham, UK

[2]Institute of Biophysics, Imaging and Optical Science (IBIOS), University of Nottingham, University Park, Nottingham, UK

E-mail: eexfap@nottingham.ac.uk

Abstract. Mechanical imaging and characterisation of biological cells has been a subject of interest for the last twenty years. Ultrasonic imaging based on the scanning acoustic microscope (SAM) and mechanical probing have been extensively reported. Large acoustic attenuation at high frequencies and the use of conventional piezo-electric transducers limit the operational frequency of a SAM. This limitation results in lower resolution compared to an optical microscope. Direct mechanical probing in the form of applied stress by contacting probes causes stress to cells and exhibits poor depth resolution. More recently, laser ultrasound has been reported to detect ultrasound in the GHz range via Brillouin oscillations on biological cells. This technique offers a promising new high resolution acoustic cell imaging technique. In this work, we propose, design and apply a thin-film based opto-acoustic transducer for the detection in transmission of Brillouin oscillations on cells. The transducer is used to generate acoustic waves, protect the cells from laser radiation and enhance signal-to-noise ratio (SNR). Experimental traces are presented in water films as well as images of the Brillouin frequency of phantom and fixed 3T3 fibroblast cells.

1. Introduction

Mechanical characterisation of biological cells is of great interest, as their properties (like stiffness or elasticity) are mostly unknown and can be the basis for mechanical modelling. Moreover, it provides an alternative mechanism for contrast which could provide new insights into cell biology. This kind of characterisation can be performed on a cell by applying stress and measure the deformations directly, with for example, an atomic force microscope (AFM) tip [1], by optical trapping [3] or micropipette aspiration [4]. Those approaches have the advantage that measurements are obtained directly. However, these are invasive techniques which can easily stress or damage a cell. Alternatively, ultrasound has been used to perform such measurements. Using a scanning acoustic microscope (SAM), mechanical images of living cells have been reported [5] as well as maps of the speed of sound [6]. Ultrasound is less invasive and features can be resolved beyond the surface. The SAM output depends on two or more parameters meaning that the quantitative measurements are not obtained directly and its resolution is typically lower than that of optical systems.

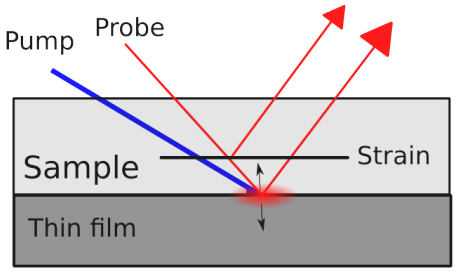

Figure 1: Schematic of Brillouin scattering detection. The light scattered at the acoustic wave interferes with the reference beam reflected from the metal film producing Brillouin oscillations.

Ultrasound is a promising way of high frequency non-destructive imaging. The speed of sound being significantly slower than the speed of light makes the acoustic wavelength comparable to the optical wavelength when ultrasound is in the GHz range. However, conventional methods to generate ultrasound are limited by the high attenuation of sound at GHz frequencies. Also, electronics and piezoelectric transducers become increasingly difficult to make in this regime. Frequencies used in a SAM to image biological cells are of the order of 1GHz and having typical wavelength of approximately $1.5\mu m$ which is lower than that used on an optical microscope.

Laser ultrasound offers a way to generate and detect high frequency ultrasound [7]. It is a non-contact, wireless, couplant-free technique capable of producing acoustic waves of very high frequency (up to THz [8]). Also, the pump-probe technique [9], it provides a mean to detect very high frequencies without the use of special detectors or electronics. Recently, picosecond laser ultrasound measurements have been performed on single biological cells [10]. The detection method presented in [10] is based on Brillouin scattering which provides a direct measure of the speed of sound and the refractive index on translucent materials. In this method, the beam scattered by a GHz acoustic wave is combined with a reference which causes an intensity modulation called Brillouin oscillations (see figure 1). The frequency of these oscillations is know as the Brillouin frequency and, for normal incidence, it is given by the relation:

$$f_B = \frac{2n\nu}{\lambda} \tag{1}$$

where ν is the speed of sound, n the refractive index and λ the optical wavelength. If the refractive index is known, the speed of sound, which is related to the mechanical properties, can be easily calculated. Moreover, the interrogated acoustic wavelength is half of the optical one used to probe the ultrasound. This technique has being demonstrated on vegetal [10], bone [11] or HeLa cells[12]. A shift in the Brillouin frequency from cytoplasm to nucleus was found indicating good contrast within a cell. The Brillouin frequency has also been used to measure the speed of sound and elasticity of biological cells[11]. However, this technique has not been applied for imaging which could be a step towards high-resolution acoustic microscopy. The main limitations to perform such imaging are given by the slow acquisition speed of the pump-probe technique, direct exposure of the cell to laser beams and poor signal to noise ratio (SNR). Low SNR is due to several factors; the limitation of used power due to the sensitivity of a cell to laser light, high losses in the detection path of a pump-probe system and the distortion of laser spots caused by light beams travelling through a heterogeneous scattering object(the cell itself).

We present a three-layer thin-film transducer designed for the detection of Brillouin scattering in transmission. The transducer serves as a shield to reduce laser light exposure while enhancing SNR. Moreover, the acquisition speed is increased by the use of a pump-probe ASOPS system [13]. These allowed to perform imaging of the Brillouin frequency of phantom and fixed cells.

2. Design of thin-film transducers for the detection of Brillouin scattering in transmission

Thin film transducers are used in this work for the generation of acoustic waves. The transducers consist of three thin layers of gold, indium tin oxide (ITO) and gold (see figure 4). The transducers were originally designed to improve the sensitivity to compression waves in picosecond laser ultrasound experiments [2] and have been re-engineered for the detection of Brillouin scattering in transmission. The wavelengths used in our pump-probe system, for generation (λ_{pump}=390nm) and detection (λ_{probe}=780nm) of the acoustic waves, govern the choice of materials; the gold films strongly absorb at λ_{pump} while reflecting/transmitting at λ_{probe} allowing flexibility of design.

Detection in transmission is the main feature of the transducers presented here since it protects the cells from laser light while increasing SNR to obtain images. This is done by exposing the lasers to the transducer through a glass coverslip and detecting the probe after it is transmitted through the sample. This increases detection levels and reduces loss of spot quality. Moreover, it gives the opportunity to increase laser power without compromising the integrity of the cells.

For that to be possible, it is necessary to optically model the transducers in order to optimise transmission (for detection) and absorption(for generation). Additionally, when the transducer is exposed to a short light pulse, it resonates not only optically but acoustically as well. The frequency of this mechanical resonance, which depends on the characteristics of the layers, has implications on the design. In this section, optical and mechanical models will be presented for the design and characterisation of the transducers.

2.1. Optical characterisation

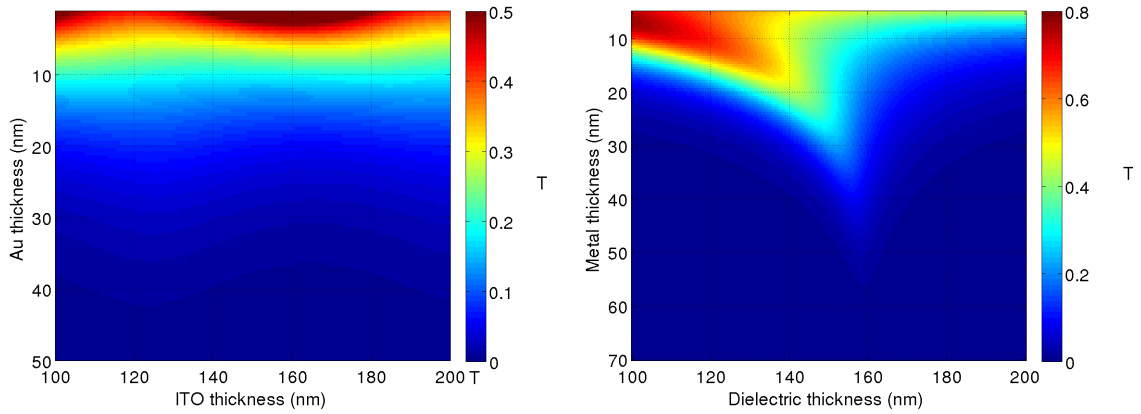

Figure 2: Simulation of the optical transmittance of the transducers for gold layers from 5-70nm and ITO layers from 100-200nm. (a) The transmittance for λ_{pump}. (b) The transmittance for λ_{probe}.

The transducers consist of an optical cavity with partially reflecting layers similar to a low order Fabry-Perot interferometer. When the transducer is exposed to light, part of the beam enters the cavity and it is resonantly transmitted and reflected. The transducer has a sensitivity to incoming waves that depend on the wavelength and dimensions of the layers [2]. Based on Fresnel coefficients, a model was created with the assumption of infinite width of the plate which is a fair approximation given the width is greater than the optical wavelength. The model

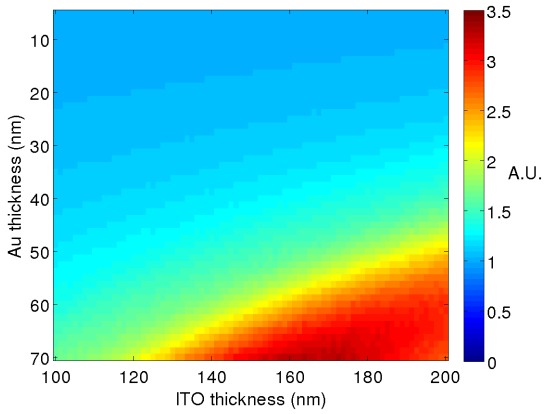

Figure 3: Simulation of the amplitude generated by the transducer at ∼5.5GHz (approximately the Brillouin frequency for a cell at λ_{probe}). The amplitude shows little change in the zone transducers are expected to be built (∼20nm of gold and ∼140nm of ITO). The increase in amplitude observed for the thicker layers is due to the resonance of the transducer shifting down to 5.5GHz.

calculates transmission at λ_{probe} and λ_{pump} assuming identical gold layer thicknesses. Figure 2 shows the result of the model. From figure 2a it is possible to see that the transmittance at λ_{pump} shows little change against ITO which means all the absorption occurs within the gold layers. Figure 2b shows that transmittance of λ_{probe} experiences a resonant peak as the ITO layer changes allowing high transmittance for relatively thick gold layers.

2.2. Mechanical Characterisation

Using finite element modelling (FEM), the transducers were modelled using a coupled optical-thermal-mechanical one dimensional model to predict the displacement resultant from optical pulse excitation. The output of the model, which consists of the displacement of the layers, is used to calculate the main resonance frequency as well as the generated amplitude at the expected Brillouin frequency from a cell (∼5.5GHz). The natural resonant frequency of the device, which is expected to be detected, changes from 6-18GHz over the range presented in figure 3 and ∼9-11GHz for the dimensions the transducers are expected to be built(∼20nm of gold and ∼140nm of ITO) [2]. Figure 3 shows a simulation of the generated amplitude at 5.5GHz for the same layer thicknesses presented in figure 2. A small variation in the generated amplitude is observed for transducers with gold layers below 50nm. For devices with gold layers above 50nm, the amplitude increases significantly because the resonant frequency of the transducer shifts down closer to 5.5GHz.

2.3. Transmission detection and design criteria

The transducers are intended to be used to protect cells against laser radiation while enhancing signal-to-noise-ratio. Figure 4 shows the proposed detection method. Lasers are incident on the transducer through the glass substrate keeping laser spots from distorting. Ultrasound is optically generated while the cell remains protected from pump radiation (beam not shown for clarity) which allow extended exposure for imaging. This transmission configuration also simplifies the detection path since only a few elements are required to capture the probing light. This simplification reduces the detection path losses in comparison with a conventional reflection mode path where polarising optics are used to separate beams travelling in opposite directions.

The design of the transducers is a compromise between optical and acoustical performance. From figure 2a, we can see that above 20nm thickness of gold, the pump transmittance at λ_{pump} is ∼0.1 which ensures a reduction of the amount of light the cell is exposed to while absorption is high for acoustical generation (not shown). Thicker gold layers would absorb even more pump light, however transmittance of λ_{probe} would be compromised. Figure 2b shows that the transmittance at λ_{probe} can be up to 0.3 for gold layers of approximately 20nm if the thicknesses

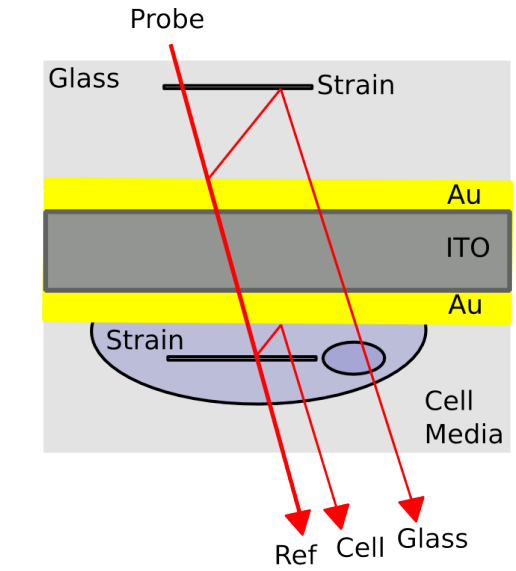

Figure 4: Schematic of the detection of Brillouin scattering in transmission based on thin-film transducers. This approach helps reduce the exposure of the cell to laser light while increasing SNR. Due to high transmittance of the film, two Brillouin signals are expected one scattered from the sample(ref+cell) and another one from the substrate(ref+glass).

of ITO is selected round the peak in transmission(∼140nm).

Mechanically, thicker gold layers can increase the amplitude of the generated wave at 5.5GHz (see figure 3). This condition could increase the amplitude of the detected signals in our experiments. Unfortunately, is not possible to take advantage of this effect at our current probing wavelength since the the thicknesses required to increase the generated amplitude (gold layers greater than 50nm) are not suitable for high optical transmission (see figure 2). Moreover. to match the generated acoustic frequency with the aimed Brillouin frequency (∼5.5GHz) brings a practical problem as becomes difficult to separate those signals from the acquired time traces.

The sound waves generated on the transducer travel through the sample and glass substrate and since the transmittance is high, meaning a second Brillouin signal from the glass is observed. As the glass substrate is considerably stiffer than most cells, the detected Brillouin frequency from the glass substrate can be easily separated from the rest of the signal by digital filtering.

Taking into consideration the models shown in this section, a transducer with 20 +/-5nm and 145+/-15nm of gold and ITO layer thicknesses respectively, is suitable for detection of Brillouin scattering in transmission. The device will have a resonating frequency of approximately 9-11Ghz [2] which is easy to separate, in the frequency domain, from the Brillouin signal. A 0.25-0.4 transmittance for λ_{probe} allows a good detection level with a reduced input power at the sample (that depends on experimental set-up). For λ_{pump} an approximate absorption of 0.4 means good light to sound conversion and a 0.1 transmittance means reduced exposure to the pump beam that biological cells are most sensitive to.

Reduction of the intensity that the cells are exposed to at λ_{pump} allows a raise in pump power, a reduction of the number of averages and an increment of the number of measurements. That leads to greater SNR, faster acquisition speed and the acquisition of an image. At the same time, the transducer transmits a portion of the probe beam to allows grater detection levels compared to a conventional reflection mode set-up. The configuration proposed here is particularly useful in the case of the sample being a biological cell, where the delicate subjects are easily affected by laser light.

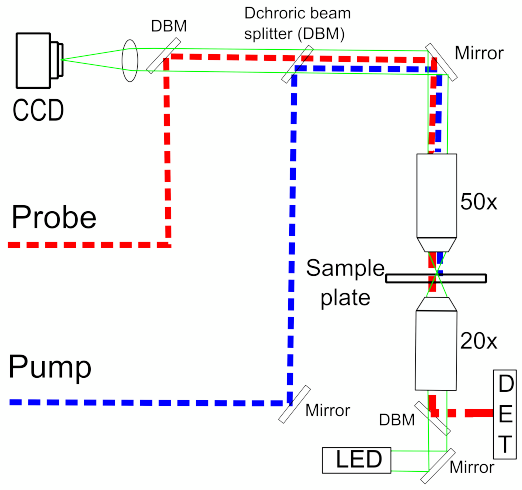

Figure 5: Schematic of the Experimental set-up. Two pulsed lasers paths are combined by dichroic beam splitters and focused to the sample with a 50x long working distance objective. The probe beam is captured by a 20x objective. Optical imaging of the sample is done in parallel to the acoustic imaging.

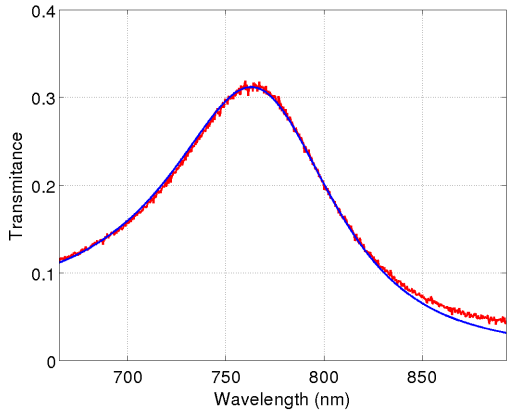

Figure 6: Fitting of theoretical and experimental transmittance of a transducer with ∼22nm gold layer thickness. The matching ITO layer thickness is 144nm. The transmittance for λ_{probe} and λ_{pump} are 0.3 and less than 0.1 respectively. The experimental measurement is represented by a red curve while the theoretical calculation by a blue curve.

3. Experimental Results

3.1. Experimental set-up

Figure 5 shows a simplified schematic of the experimental set-up. The experiment is based on a dual laser ASOPS system [13]. The lasers consist on two 780nm, 150fs pulsed lasers with a repetition rate of 100MHz (10ns measuring window). This kind of system allows the tuning of the repetition rate of one of the lasers (probe) while locking its phase with respect to the other laser (pump). This allows the delay between the pulses to be set and swept without the need of a mechanical delay line. This provides a great simplification of the experimental set-up while increasing the acquisition speed. By having a 10kHz difference in repetition rate between the lasers, one full trace is acquired every 100μs. This means that it is possible to acquire up to 10k traces per second if the acquisition system is fast enough.

The pump laser is frequency doubled in a non linear crystal to 390nm. Both beams are combined by the use of a dichroic beamsplitter and focused on to the sample by a 50x long working distance objective. The probe beam is captured below the sample by a 20x long working distance objective and redirected to the detector by a dichroic beamsplitter that allows illumination for optical imaging on a CCD. The system typically uses 1mW average power for λ_{probe} and 0.5mW for λ_{pump} which corresponds to pulse energies of 10pJ and 5pJ respectively.

3.2. Brillouin scattering detection in transmission

The transducers were constructed by sputter coating the layers and their transmission was measured to compare it with a modelled one. As seen in figure 6, there is a good fit between theoretical and experimental results. ∼0.3 transmission was reached for a device with ∼20-140-20nm of gold-ITO-gold. For this device a ∼27% of the input light makes it to the detector. This is almost three times more light compared to the ∼0.1 of light returning on the reflection path in our system. This reduction in losses improves the SNR for the same amount of probe power coming out of the objective. Moreover, if the same probe power is going through the specimen by compensating the power coming out of the objective, the detection levels are significantly better for the transmission case since the losses in the path to the detector are smaller.

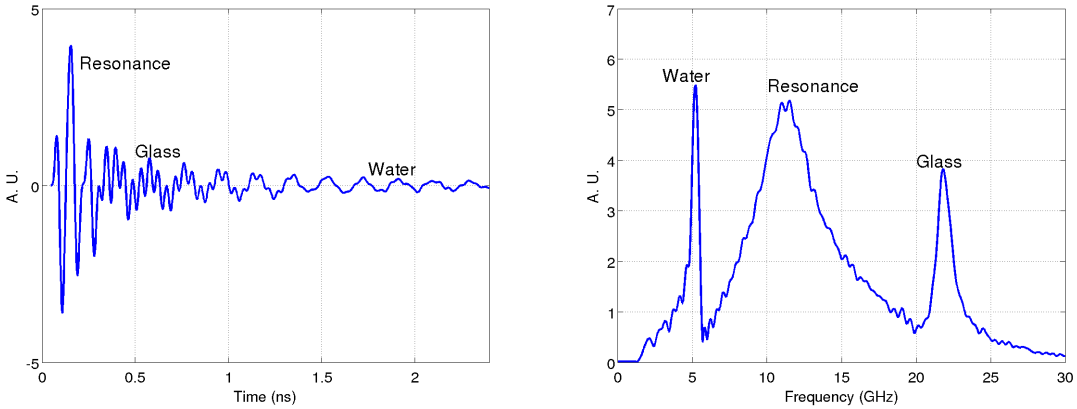

(a) **(b)**

Figure 7: Sample of experimentally detected time traces from a water film in transmission using thin-film transducers. (a) Time trace where three signals are present; transducer response which decays quickly(∼0.3ns) , the high frequency Brillouin oscillation from the glass substrate(∼22GHz) and a low frequency Brillouin oscillation from the water film (∼5GHz). (b) The Fourier transform showing the Brillouin peaks from the different signals.

A water film was used to test our approach due to its similarity to the cell media. The two Brillouin signals expected in these experiments from scattered light in the specimen and the glass substrate, are shown in figure 7. The mechanical resonance of the transducer is also detected due to the optical sensitivity of the transducer [2]. The time trace on figure 7a shows the change in instantaneous intensity of the probe beam as a result of the exposure to a pump pulse. There, the raw time trace was processed to remove the thermal background. On figure 7b, the Fourier transform of the trace in figure 7a is shown. The two sharp peaks correspond to the Brillouin oscillations in water (∼5GHz) and glass (∼22GHz). The additional broad peak is the device resonance which is due to the change in cavity size induced by the generated acoustic wave. The unwanted Brillouin component in the glass can be removed by digital filtering. The device resonance could be removed in a similar way or as it only last ∼0.3ns, could be also removed by truncation.

3.3. Brillouin imaging of polystyrene phantoms

Before imaging a real cell, an experiment on phantom cells made out of melted lumps of 5μm polystyrene beads was performed. This provides a well known homogeneous specimen to test our approach. The beads were deposited on a transducer and then heated to 245 degrees centigrade for approximately 30 minutes to melt them. This leaves structures that resemble the shape of a

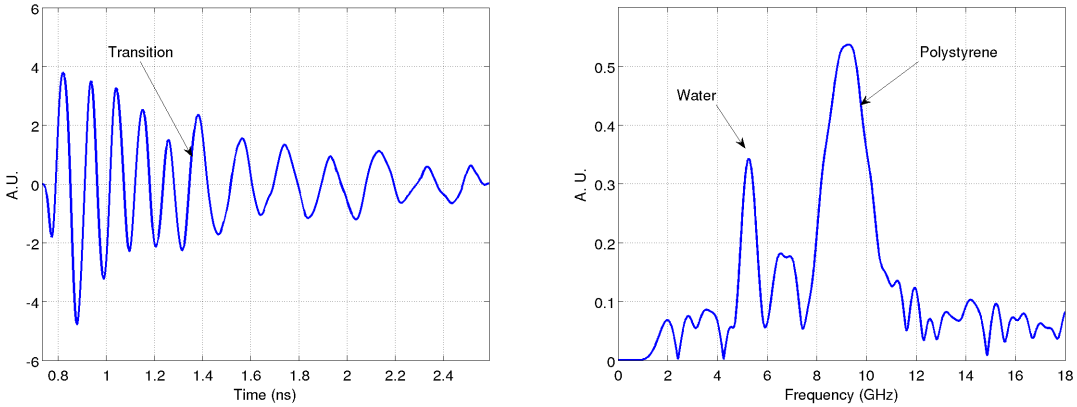

(a) **(b)**

Figure 8: Sample of experimentally detected traces in transmission using thin-film transducers on a polystyrene phantom cell. (a) Time trace where two frequencies are present; the high frequency Brillouin oscillation from the polystyrene phantom(∼9GHz) and a low frequency Brillouin oscillation from the water surroundings (∼5GHz). (b) The Fourier transform showing the spectral separation between the Brillouin peaks coming from the phantom and the medium.

cell and ensures good attachment to the transducer. The fabricated phantoms were submersed in water to simulate the presence of cell media that gives a background reference for contrast. The sample was mounted on a sealed chamber with the phantom facing the transmission objective (20x). Figure 8a shows an example of a time trace from a polystyrene phantom. There, it is possible to see the Brillouin frequency shifting from high frequency (9GHz) to low frequency (5GHz) when the sound leaves the phantom and enters the water. This transition is an indication of the phantom thickness at that particular point. The large difference in properties from water to polystyrene makes the transition easy to see however in the case of a real cell, the shift of the Brillouin Frequency will be much smaller.

Figure 9 shows an image of the Brillouin frequency of a polystyrene phantom. The scan consisted of 441 points covering 40 by 40μm in 2μm steps. The scan lasted approximately one hour taking 30k averages per point. A time trace was obtained at each point and its Brillouin frequency evaluated by performing a Fourier transform. Figure 9a shows an optical picture of the polystyrene phantom; the shape of the polystyrene beads is still visible. In figure 9b the Brillouin frequency map of the phantom shows good correlation with the optical picture. The variation of the Brillouin frequency within the phantom is small suggesting good homogeneity. If the refractive index in the phantom is constant (1.58 [14]), the speed of sound on the polystyrene obtained from equation 1 is approximately 2200 m/s, similar to the 2400m/s bulk speed reported by Smith et al [15].

3.4. Brillouin imaging of fixed cells

As demonstrated in the previous section, the approach presented in this work is viable. However, there are significant differences for a real cell; the Brillouin shift in the cell-media boundary is much smaller having the effect of reducing contrast. Also, the thickness of a cell is highly variable from sub micron in the edges to several tens of microns in the centre. These conditions make a cell a challenging subject.

3T3 fibroblast cells were selected for imaging due to their availability and their suitable dimensions. The transducers were pretreated with Poly-L-lysin, then the cells were seeded on

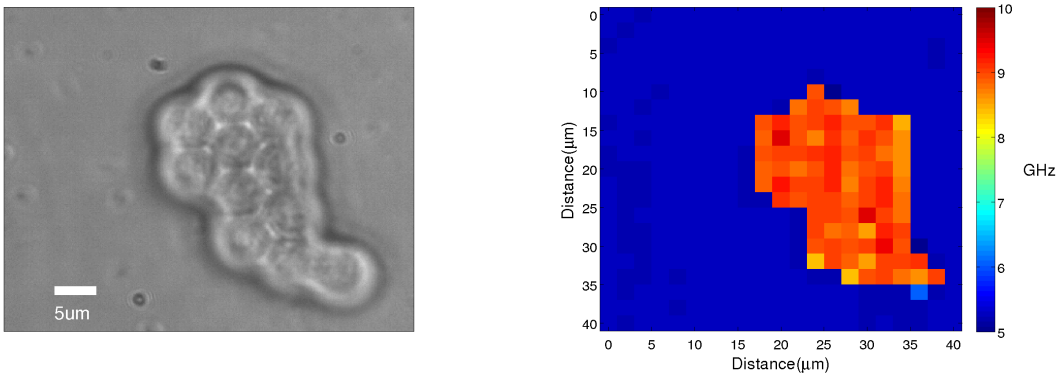

(a) **(b)**

Figure 9: Image of the Brillouin frequency of a phantom cell. (a) Optical picture of the phantom cell where the beads used to build it are partially visible. (b) The Brillouin map of the phantom cell. The correlation between optical and Brillouin frequency is good. There is large Brillouin frequency shift (∼4GHz) due to the difference in material properties between polystyrene and water.

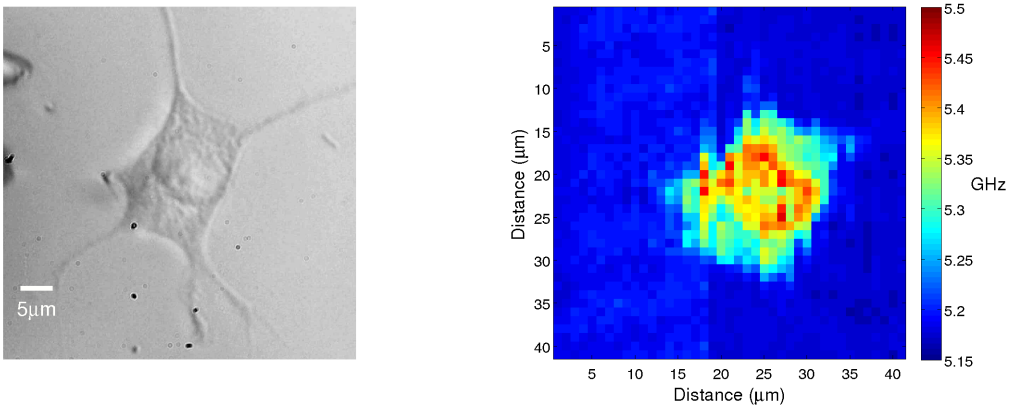

(a) **(b)**

Figure 10: Image of the Brillouin frequency of a fixed cell. (a) Optical picture of the fixed cell under examination. (b) The Brillouin map of the fixed cell. The correlation between the optical and Brillouin frequency image is good. The Brillouin frequency change in the cell is small (∼20-250MHz) due to the similarity in mechanical properties between cell and medium.

them and fixed a day later. By assembling a two coverslip chamber (Live Cell Instruments Inc. chamilde CF-T) media was able to be pumped preventing bubble formation. Using the same scanning parameters and laser powers as the phantom case, an image of a fixed 3T3 cell was obtained. Figure 10 shows a fixed 3T3 fibroblast cell and its Brillouin frequency map. The correlation of the optical image with acoustical one is good. The features shown inside the cell in figure 10b are likely to be real changes in the properties of the cell. The measured Brillouin frequencies in the cell were between 5.25 and 5.5GHz with 50 and 250MHz shift from the Brillouin frequency of the background. Taking into consideration a refractive index of 1.36 [16] and assuming it is constant over the cell, the speed of sound in the cell changes from 1548 to 1605 m/s. Near the edges of the cell, the features are hard to see mostly because the signal lasts

for a very short time and the signal from the media dominates the Fourier transform response.

4. Discussion

Since it is possible to observe when the sound waves leave the specimen and enter the water, it is also possible to calculate the thickness of the specimen if the speed of sound of is known. By knowing the refractive index before hand, it is easy to calculate the speed of sound using the Brillouin frequency. This opens the opportunity to not only measure the speed of sound but also to obtain the profile of the sample provided that the penetration depth of the acoustic wave is large enough to reach the boundary of a given object. It would be also possible to determine whether the cell is attached to the substrate or not.

Pulsed lasers emit continuously a train of pulses whether the acquisition system is ready or not. If the acquisition system is not ready to capture another set of traces when the trigger signal is received, then the signal is ignored and the specimen is exposed unnecessarily to laser light. The acquisition system could be busy processing data, sending it to a hard drive or simply waiting for the stages to move. Whatever the case our system can handle only approximately 30% of the pulses leaving the rest to be unnecessarily exposed to the specimen. There is an opportunity to improve this by blocking the pulses when the system is not ready and/or increasing the capabilities of the acquisition system and hence the capability of imaging a object which is changing in time.

The technique presented here could be extended for imaging living cells. However, the fragility of living cells introduces much stricter requirements on the light and heat doses delivered to the cells than those for fixed or phantom cells presented here. The thin film transducers presented in this paper go a long way to managing the light and heat load, but additional improvements can be made. With regards to light shielding, the current transducer blocks around 90% of the pump laser which allows images to be taken, but by changing the materials used for the dielectric layer (for example using SiO2), the transmission at the pump wavelength can be reduced (5%) giving greater protection for the cell . Heat exposure can also be reduced by the use of a different substrate with a higher thermal conductivity. For instance, sapphire offers 30 times higher thermal conductivity than a typical glass cover slip promoting better dissipation of heat and thus lower peak temperatures at the laser spot focus. These modifications will allow Brillouin oscillation images to be taken of living cells

4.1. Summary

In this paper images of the Brillouin frequency on phantom and fixed cells were presented by re-engineering thin film transducers [2]. The detection of Brillouin scattering in transmission was proposed and successfully applied to perform picosecond laser ultrasound experiments on delicate cultured cells. The approach is particularly useful for cells because the transducer itself act like a shield against pump laser light radiation while enhancing SNR. Brillouin frequencies measured on fixed 3T3 fibroblast cells were between 5.25 and 5.5GHz to calculate speed of sound from 1548 to 1605m/s which are similar to previously reported results on HeLa cells using a SAM (at 0.86GHz) [17] and on vegetal cells using Brillouin scattering detection [10].

References

[1] Kuznetsova et al 2007 *Micron* **137** 219
[2] Smith, Richard J. and Cota, Fernando Perez and Marques, Leonel and Chen, Xuesheng and Arca, Ahmet and Webb, Kevin and Aylott, Jonathon and Somekh, Micheal G. and Clark, Matt 2015 *JASA* **38** 824
[3] Nawaz et al 2012 *PloS one* **7** e45297
[4] Hochmuth, R M 2000 *J. Biomech* **33** 15
[5] Hildebrand, J A and Rugar, D and Johnston, R N and Quate, C F 1981 *Proc. Natl. Acad. Sci.* ***U S A*** **78** 1656
[6] Kundu, T and Bereiter-Hahn, J and Karl, I 2000 *Biophys. J.* **78** 2270

[7] Scruby, C.B and Drain, L.E 1990 *Laser Ultrasoncs Thecniques and Applications* (New York: Taylor and Francis Group) p 433
[8] Maznev, A A and Manke, Kara J and Lin, Kung-Hsuan and Nelson, Keith A and Sun, Chi-Kuang and Chyi, Jen-Inn 2012 *Ultrasonics* **52** 1
[9] Thomsen, C. and Grahn, H.T. and Maris, H.J. and Tauc, J. 1986 *Opt. Commun.* **60** 55
[10] Rossignol, C. and Chigarev, N. and Ducousso, M. and Audoin, B. and Forget, G. and Guillemot, F. and Durrieu, M. C. 2008 *Appl. Phys. Lett.* **93** 123901
[11] Ducousso, Mathieu and El-Farouk Zouani, Omar and Chanseau, Christel and Chollet, Céline and Rossignol, Clément and Audoin, Bertrand and Durrieu, Marie-Christine 2013 *EPJAP* **61** 11201
[12] Dehoux, T. and Audoin, B. 2012 *JAP* **112** 120702
[13] Elzinga, Paul A and Lytle, Fred E. and Jian, Yanan and King, Galen B. and Laurendeau, Normand M. 1987 *Appl. Spect.* **41** 2
[14] Xiaoyan Ma and Jun Q Lu and R Scott Brock and Kenneth M Jacobs and Ping Yang and Xin-Hua Hu 2003 *PMB* **48** 4165
[15] D. M. Smith and T. A. Wiggins 1972 *Appl. Opt.* **11** 2680
[16] Lanni, F and Waggoner, A S and Taylor, D L 1985 *J. Cell Biol.* **100** 219
[17] Weiss, Eike and Anastasiadis, Pavlos and Pilarczyk, Gotz and Lemor, Robert and Zinin, Pavel 2007 *IEEE UFFC* **54** 2257